Journal of Coating Science and Technology, 2014, *1*, 78-87

Journal of Coating Science and Technology
http://www.lifescienceglobal.com/journals/journal-of-coating-science-and-technology

The Effects of Primary Oxy-Salts on Anodizing Magnesium Alloy AZ91D

Dingchuan Xue[a,#], Yeoheung Yun[b,*], Brian H. Halsall[c], William Vanooij[a,d], Mark J. Schulz[e] and Vesselin Shanov[a]

[a]*Dept of Chemical and Materials Engineering, University of Cincinnati, Cincinnati, OH 45221, USA*

[b]*Dept of Bio-Engineering, North Carolina Agricultural & Technical State University, Greensboro, NC 27411, USA*

[c]*Dept of Chemistry, University of Cincinnati, Cincinnati, OH 45221, USA*

[d]*Ecosil Technologies LLC, Fairfield, OH 45014, USA*

[e]*Dept of Mechanical Engineering, University of Cincinnati, Cincinnati, OH 45221, USA*

Abstract: Anodization is known to be an effective way to slow down the initial corrosion rate of magnesium (Mg) and its alloys. Here, we investigated the specific use of oxy-salts to improve the corrosion resistance of anodizing coatings. Oxy-salts of silicate, phosphate, and carbonate were added separately to a sodium hydroxide alkaline electrolyte used to anodize Mg alloy AZ91D. The process was investigated in terms of anodizing behavior, the surface properties, and the corrosion behavior of AZ91D. Anodizing AZ91D using the silicate- containing electrolyte generated sparks, and produced a thicker and more corrosion-resistant layer than the other oxy-salts. In the process, MgO and SiO_2 formed Mg_2SiO_4 at high temperatures. Coatings from the phosphate- and carbonate- containing electrolyte anodizations did not contain phosphorus or carbon. We also studied the effects of silicate concentration on the corrosion resistance and properties of the surface.

Received on 02-03-2014
Accepted on 01-05-2014
Published on 07-07-2014

Keywords: Anodization, corrosion, AZ91D, primary oxy-salt.

DOI: http://dx.doi.org/10.6000/2369-3355.2014.01.01.9

1. INTRODUCTION

With excellent mechanical properties, lightweight magnesium (Mg) and its alloys have become popular candidates for industrial applications. Recently, Mg is also being evaluated as an implant material due to its biodegradability, biocompatibility, and bone-like physical properties [1-4]. In industrial and biological applications, the low corrosion resistance of Mg is a drawback since Mg loses strength and toughness when it corrodes. In biomedical applications, Mg implants may degrade too quickly, especially at the initial stage of implantation. Therefore, corrosion protection is needed when Mg is considered for industrial and biomedical applications.

Anodization is one of the effective approaches used to slow down the corrosion rate of Mg. Many studies have investigated various aspects of anodization of Mg including the effects of different substrate materials [5-7], anodizing process parameters [7-9], and electrolytes [9-11]. Currently, alkaline electrolyte is used most. Popular additives to the alkaline electrolyte are fluoride [10, 12], metallic salts [13-15], and oxy-salts such as silicate, phosphate, carbonate, and borate [13, 14, 16-19]. The additives form insoluble Mg compounds, such as Mg oxide and hydroxide, on the surface of the Mg, improving its corrosion resistance [8, 20, 21]. However, previous studies used chemical mixtures, and the effects of specific chemicals have been given sparse attention. Chai *et al*. [22] investigated the specific addition of silicate, phosphate, aluminate and molybdate as secondary oxy-salts in addition to the primary oxy-salt of borate in the alkaline electrolyte. However, few studies have examined the effects of adding silicate, phosphate, and carbonate on anodizing Mg as the primary oxy-salt. Here, sodium silicate, sodium phosphate, and sodium carbonate were added separately as the primary oxy-salts to a sodium hydroxide alkaline electrolyte, and compared. The concentration of

*Fort-IRC Building Room # 119, 1601 E. Market St, Greensboro, NC 27411, USA; Tel: 001-336-256-1151 ext. 2010; Fax: 001-336-256-1153;
E-mail: yyun@ncat.edu

#Currently holding a position at TDK Headway Technologies Inc.

Table 1: Anodization Systems and Symbols Used in this Work

Symbols	Electrolyte		Anodizing parameters	
	Composition	pH	Current (mA/cm^2)	Time (min)
A0	2 M NaOH	13.02	10	30
A1	2 M NaOH + 0.05 M Na_2SiO_3	13.02	10	30
A2	2 M NaOH + 0.05 M $Na_3PO_4 \cdot 12\ H_2O$	13.02	10	30
A3	2 M NaOH + 0.05 M $Na_2CO_3 \cdot 10\ H_2O$	13.02	10	30
A1	2 M NaOH + 0.05 M Na_2SiO_3	13.02	10	30
A1-1	2 M NaOH + 0.15 M Na_2SiO_3	13.16	10	30
A1-2	2 M NaOH + 0.5 M Na_2SiO_3	13.2	10	30
A1-3	2 M NaOH + 3 M Na_2SiO_3	13.9	10	30

silicate was optimized by characterizing the surface and its ability to inhibit corrosion.

2. EXPERIMENTAL

AZ91D was from ACT Test Panels Technologies, and machined into pieces 15 mm x 15 mm x 3 mm. The machined samples were embedded in epoxy resin (Buehler Inc.). The area exposed was 2.25 cm^2. The epoxy-sealed samples were then polished up to 800 grit, rinsed with ethanol and DI water, and air-gun dried before use. The machined, polished and cleaned samples are named “fresh AZ91D” in this work.

The detailed experimental solutions are listed in Table **1**, and were mixed well before use. Each prepared solution was 100 mL. The symbols for each system will be used in this paper. The power supply (0-3000 V, 0-40 mA) was from Circuit Specialist Inc. The anode (AZ91D) and cathode (platinum hoop, Fisher Scientific) were 5 cm. apart. Anodizing was done at a constant current density of 10 mA/cm^2, and the bath was stirred throughout the process. Finally, the anodized sample was rinsed with distilled water and dried with an air gun. The cell temperature and voltage were recorded.

Electrochemical tests were used to study the corrosion behavior using a 0.15 M NaCl solution as a corrosive environment at room temperature. An SR 810 frequency response analyzer and Gamry PCI4/300 potentiostat comprised the electrochemical test equipment. An Ag/AgCl in saturated potassium chloride electrode and platinum mesh functioned as the reference and counter electrodes, respectively. The distance between the electrodes was fixed during all tests. Open Circuit Potential (OCP) measurements were made 1 and 10 hrs after immersion. A range of corrosion potential, (E_{corr}) ± 0.25 V and 1 mV/s scan rate was applied in the DC polarization test. The experimental curves were fitted by the nonlinear least squares curve fitting tool, Gamry Echem Analyst, yielding the results of the corrosion potential (E_{corr}), corrosion current density (I_{corr}) and corrosion rate . The frequency used was from 10^5 Hz to 0.2 Hz in the electrochemical impedance spectroscopy (EIS) test. Several equivalent circuit models using the nonlinear least squares curve fitting tool, Gamry Echem Analyst, were tried to fit the experimental results and the best possible fit was selected. A Philips XL 30 environmental scanning electron microscope (ESEM) was used to characterize the morphology. Energy-dispersive X-ray spectroscopy (EDX) was used to investigate the chemical composition. During the EDX analysis, areas were measured at 100 X magnification, a 15 kV accelerating voltage, and 20 seconds collecting time.

The contact angle is the angle at which a liquid/vapor interface meets the solid surface. Contact angle is used to characterize and observe the coatings on metal. Contact angle measurements were carried out on a contact angle goniometer VCA2000, manufactured by AST products, Inc, Billeriaca, MA, USA. Water was injected onto the coatings by a syringe. The results of contact angle were obtained by applying goniometer software.

3. RESULTS

3.1. The Effects of Oxy-Salts on Anodization

3.1.1. The Effects on Anodization Behavior

Figure **1**, shows that A0 (A), A1 (B), A2 (C) and A3 (D) had different anodization behaviors. Low terminating voltages for A0, A2, A3 and a high terminating voltage for A1 were found. The voltages of A0, A2, and A3 immediately jumped to 7-9 V within a few seconds and then dropped to around 4 V. However, the A1 voltage increased dramatically to 60 V in a few seconds. Uniform sparking started at about 45 V.

3.1.2. The Effects on Surface Characterization

The morphology of the coating produced from the 2 M NaOH-only electrolyte is shown in Figure **2A**. Figure **2B** shows that adding silicate to the 2 M NaOH electrolyte had a strong effect on the morphology of the coating. Adding phosphate, Figure **2C**, and carbonate, Figure **2D**, barely affected the coating morphology. Adding silicate created volcano-like rough areas on the surface. The relatively rough areas had larger, but less porosity (number of pores) compared to relatively smooth areas. The rough area has about 4 pores per 4 E+04 um^2. The smooth area has about 10 pores per 4 E+04 um^2. As seen in Table **2**, all four samples of A0, A1, A2,

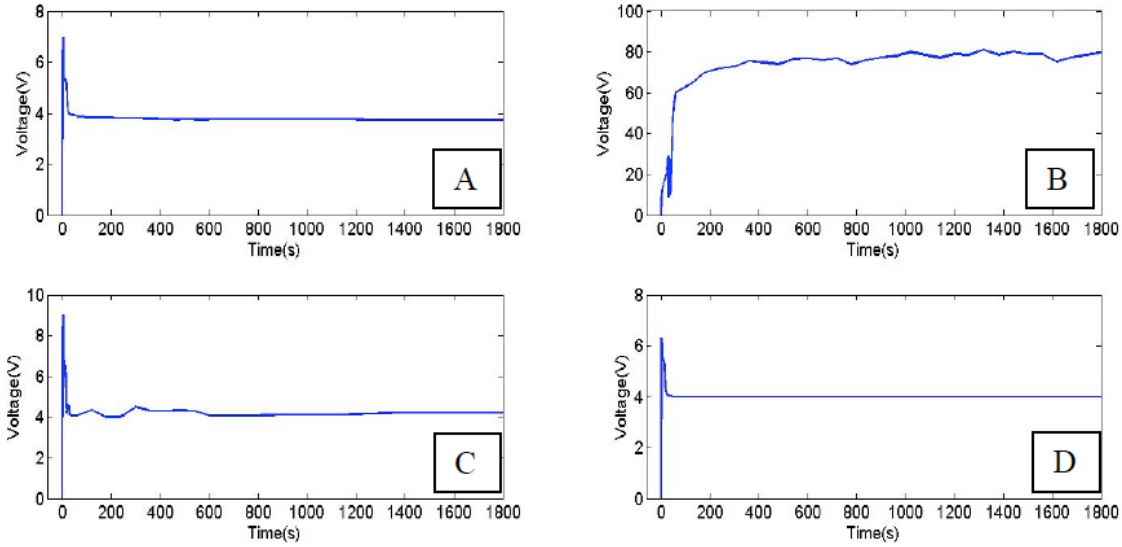

Figure 1: Anodizing behavior of different primary oxy-salts additions at 10 mA/cm^2 for 30 min. (**A**) 2 M NaOH(A0), (**B**) 2 M NaOH + 0.05 M Na_2SiO_3(A1), (**C**) 2 M NaOH + 0.05 M Na_3PO_4(A2), (**D**) 2 M NaOH + 0.05 M Na_2CO_3(A3).

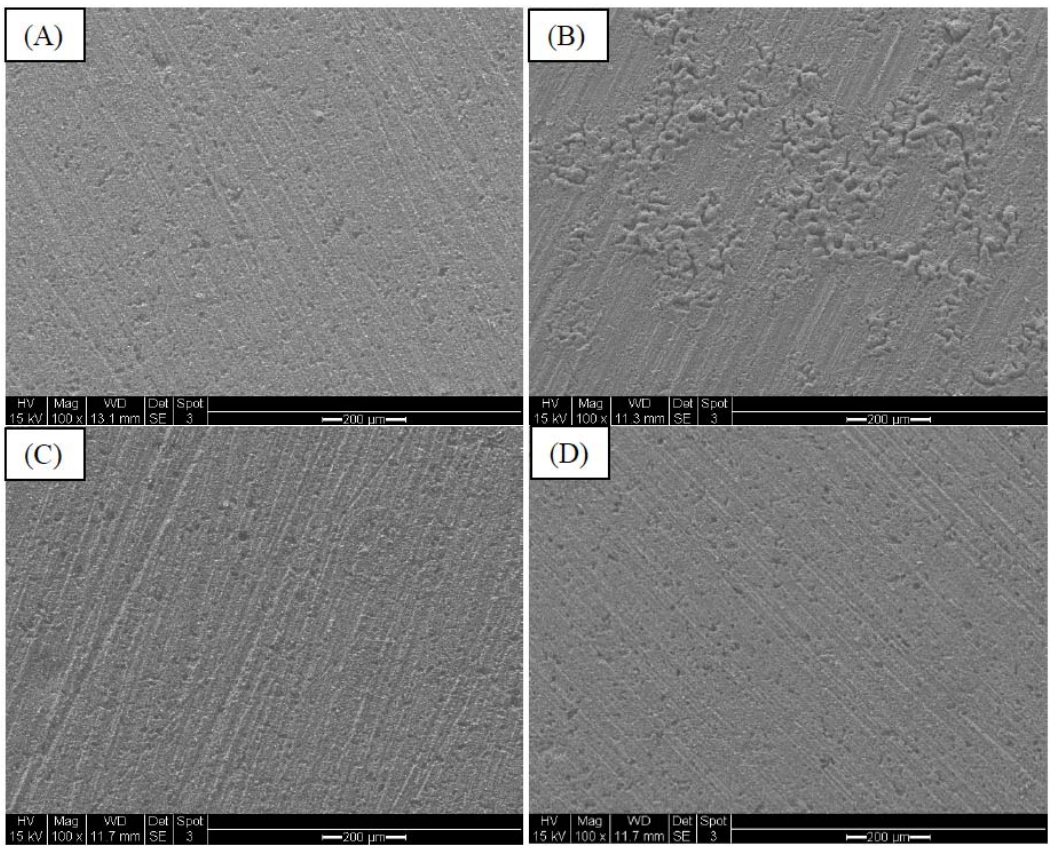

Figure 2: Morphology of anodized coatings with different primary oxy-salt additions at 10 mA/cm^2 for 30 min. (**A**) 2 M NaOH(A0), (**B**) 2 M NaOH + 0.05 M Na_2SiO_3(A1), (**C**) 2 M NaOH + 0.05 M Na_3PO_4(A2), (**D**) 2 M NaOH + 0.05 M Na_2CO_3(A3).

and A3 had similar O concentrations. Mg dropped from 85.5 at. % in the fresh AZ91D to around 50.0 at. % in the anodized samples. Si was found as 2.0 at. % in A1. P and C were not found in the A2 and A3 systems. Zn was not listed in Table **2** since it was below 1.0 at. % in the fresh AZ91D and even lower in anodized samples.

3.1.3. The Effects on Corrosion Behaviors

In Figures **3A** and **B**, all the anodized samples had higher corrosion impedances than the fresh AZ91D during the 1 hour and 10 hour EIS tests. In the first hour, Figure **3A**, all of the anodized samples are better than the untreated alloy. At certain phase angle, the absolute impedance of untreated

Table 2: Detailed Surface Element Information in Atom Percent of Anodized Coatings from Different Primary Oxy-Salts Addition Electrolytes at 10 mA/cm^2 for 30 min. Fresh AZ91D; 2 M NaOH(A0); 2 M NaOH + 0.05 M Na_2SiO_3(A1); 2 M NaOH + 0.05 M Na_3PO_4(A2); 2 M NaOH + 0.05 M Na_2CO_3(A3)

	AZ91D	A0	A1	A2	A3
O	5.2	44.6	43.2	48.7	50.3
Mg	85.5	50.3	51.3	46.6	45.1
Al	9.3	5.1	3.5	4.7	4.6
Si	-	-	2.0	-	-
P	-	-	-	-	-
C	-	-	-	-	-

samples is 560 ohms. The anodized sample with silicate additive has the highest absolute impedance that is around 2900 ohms. The other anodized samples have the absolute impedance of around 1100 ohms. However, at the low frequency region, all of the tested samples revealed the pitting corrosion sign. The imaginary impedance dropped below zero. In the 10 hour EIS test, Figure **3B**, all of the tested samples absolute impedance reduced. The anodized sample with silicate additive remains the strongest in terms of corrosion resistance. The best possible fit equivalent circuit model and corresponding schematic anodized coating structure on AZ91D after localized pitting corrosion happened were listed in Figure **3C** [23]. R_S is the solution resistance, and CPE is the constant phase element. Compared to a pure capacitor, CPE is often used to describe an imperfect coating. The anodized coating has defects and pores on the surface, and CPE was more suitable than a capacitor in fitting the curves. The impedance of CPE, Z_{CPE} is given by:

$$Z_{CPE}=Y0^{-1}(j\omega)^{-m} \quad (1)$$

Where Y0 is a constant, ω is angular frequency, j= $(-1)^{1/2}$ and m is an exponential index that represents a dispersion of relaxation. When m = 1, CPE is a pure capacitor; when m = 0, CPE is a pure resistor. The values of Y0 from Equation (1) can be used to calculate the impedance of the CPE. The

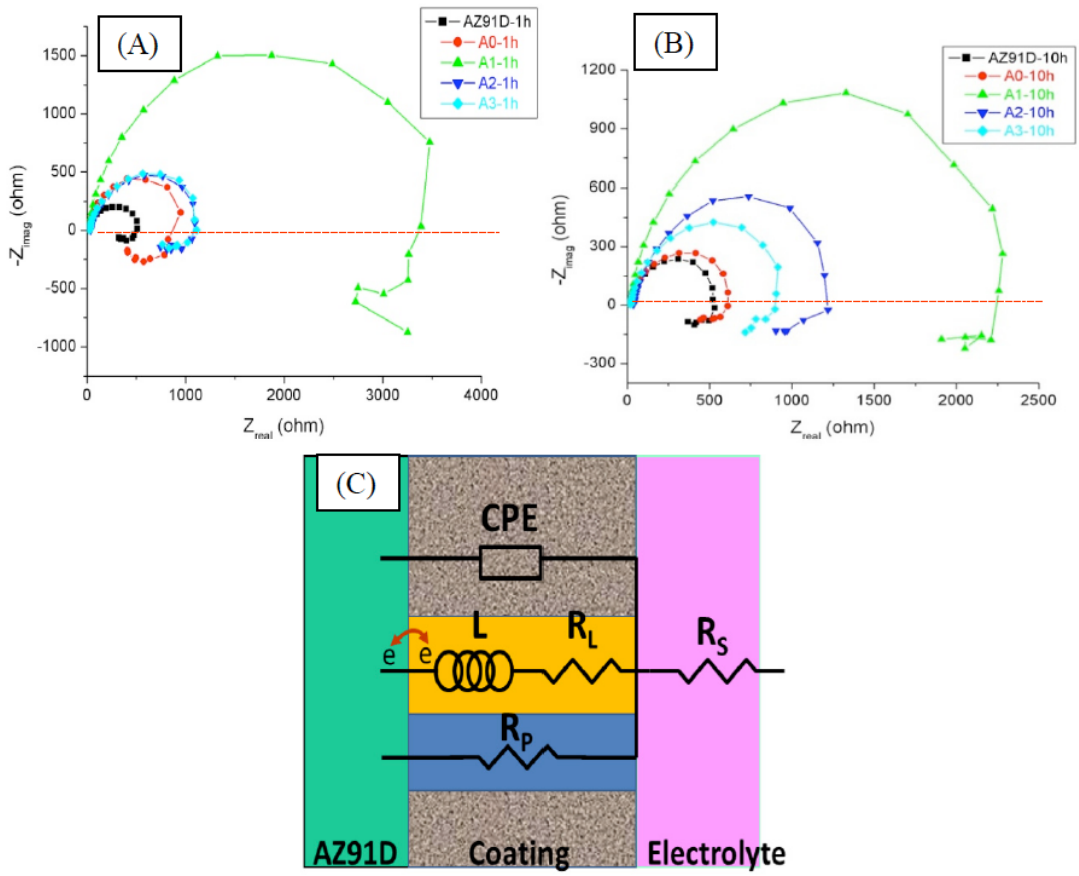

Figure 3: EIS of fresh and anodized AZ91D immersion in 0.15 M NaCl solution. (**A**) 1 hour; (**B**) 10 hours; (**C**) equivalent model circuit and corresponding schematic anodized coating structure on AZ91D after localized pitting corrosion.

Table 3: EIS Fitting Parameters of Fresh AZ91D and A0, A1 for 1 and 10 hours Immersion in 0.15 M NaCl Solution

	1 h			10 h		
	Fresh AZ91D	A0	A1	Fresh AZ91D	A0	A1
R_P (Ω)	528.1	993.7	3766	566.4	677.5	2511
R_S (Ω)	14.11	13.86	16.19	13.61	13.99	16.14
Y0 (μF)	43.7	29.2	9.2	63.7	67.3	13.3
m	0.856	0.916	0.903	0.881	0.862	0.899
L (H)	235.3	234.2	2962	435.2	460.1	2375
R_L (Ω)	660.2	535.7	6686	746.1	1083	7291

polarization resistance (R_P) is that due to pores and defects in the coating. L represents inductance. L is due to the relaxation processes involving the dissolution of metal to ions leading to the formation of corrosion products with species from electrolyte at local places of corrosion. R_L is inductance-introduced resistance.

At high frequency, solution resistance (R_S), CPE and polarization resistance (R_P) dominated the structural current flow. At low frequency, since all of the samples showed inductance loops (curves below the red dashed lines in Figure **3A** and **B**), pitting corrosion occurred. R_S, an inductance L and inductance introduced resistance, R_L, dominated the micro-structural current flow [12, 23-25]. The detailed fitting parameters are listed in Table **3**. The untreated Mg alloy, the anodized sample without additive (A0) and the anodized sample with silicate as additive (A1) are compared. During the 10 hour EIS test, before severe corrosion occurs, R_P, CPE and R_L are the important electrochemical parameters in terms of evaluating the ability to protect against corrosion. In the 1 hour test, A1 and A0 show the polarization resistance of 3766 ohms and 993.7 ohms, respectively. The untreated AZ91D shows 528.1 ohms of polarization resistance. The A1 sample shows the highest inductance introduced resistance of 6686 ohms followed by the 535.7 ohms of A0 and 660.2 ohms of untreated AZ91D. A1 also displays the lowest constant Y0 of 9.2 μF. In the 10 hour test, A1 still keeps the highest in polarization and inductance introduced resistances and the lowest in constant Y0. In this study, adding silicate (A1) produced a better protective coating, in terms of resistance and capacitance.

The DC polarization test as shown in Figure **4**, and the detailed fitting parameters listed Table **4**, carried out after 10 hours immersion in 0.15 M NaCl solution. The test was run on fresh AZ91D, A0 and A1. Anodization not only increased the corrosion potential but also reduced the corrosion rate compared to that of fresh AZ91D which is 78.01 mils per year. A1, with a corrosion rate of 5.79 mils per year, had the lowest of all.

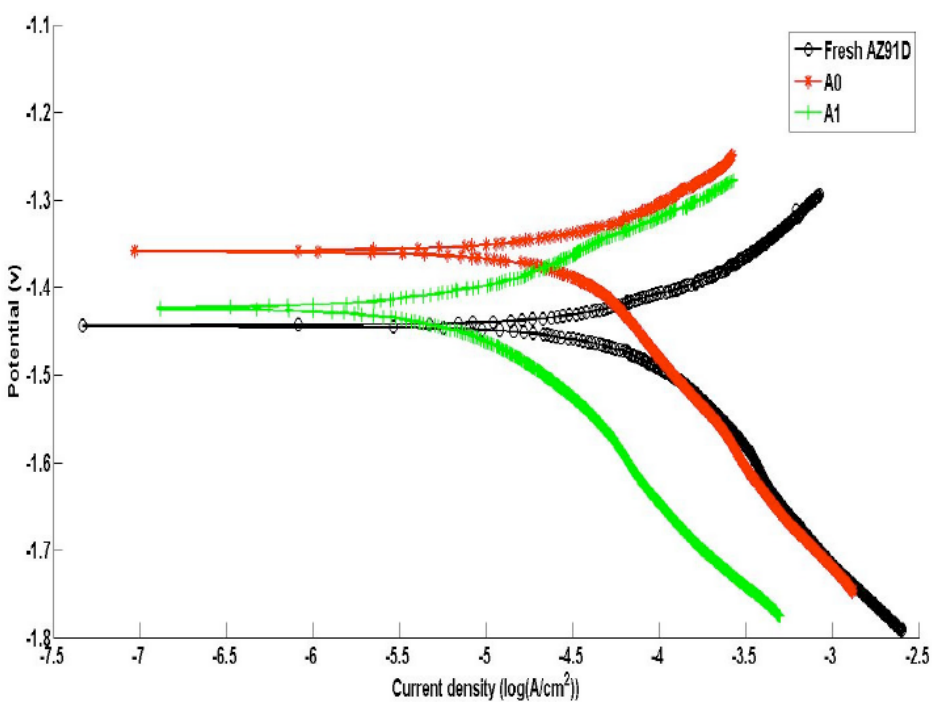

Figure 4: DC polarization test on fresh AZ91D, A0 and A1 immersion in 0.15 M NaCl solution.

Table 4: DC Polarization Fitting Parameters of Fresh AZ91D and A0, A1, A1-3 for 10 hours Immersion Time in 0.15 M NaCl Solution

	Fresh AZ91D	A0	A1	A1-3
E_{corr} (V vs Ref)	-1.44	-1.36	-1.42	-1.37
I_{corr} (uA/cm^2)	43.12	15.15	3.13	1.17
Corrosion Rate (mills per year (mpy))	78.01	27.55	5.79	2.01

3.2. The Effects of Na_2SiO_3 Concentration on Anodization

The effects of the concentration of silicate on the coating morphology are shown in Figure **5**. The silicate concentrations were 0.05 M (A), 0.15 M (B) and 0.5 M (C) to 3 M (D) added into the 2 M NaOH electrolyte. The rough areas appeared to be larger in 0.15 M than in 0.05 M. However, from 0.15 M to 0.5 M, the morphology changed dramatically. At 0.5 M addition, the surface became relatively uniform compared to the smooth-rough combination morphology. However, when 3 M was added, the morphology changed greatly, from appearing uniform-loose (0.5 M) to uniform-dense (3 M). The pore size and porosity were both reduced at 3 M, and the surface chemical elements changed with varied amounts of silicate. In Table **5**, from 0.05 M to 3 M, the O, Si, as well as Na concentration increased, and Mg and Al concentrations decreased. The increased O might be due to the formation of Mg_2SiO_4 [16, 19], instead of MgO or Mg (OH) $_2$. Since the Mg (OH) $_2$ and water concentrations were the same only the silicate concentration was varied. The increase of Na might be due to the Na^+ physically attached from electrolyte in the form of Na_2SiO_3.

The silicate concentration also affected the thickness of the coating. When 0.05 M and 0.15 M were added, the coatings were barely seen on Figure **6A** and **B**, respectively. However, as seen in Figure **6C**, when the silicate concentration reached 0.5 M, the coating was obvious at 15 μm thick. The coating also had some pores and was not uniform. When 3 M silicate was added, however, the coating appeared to be uniformly thick at 23 μm, with a dense structure.

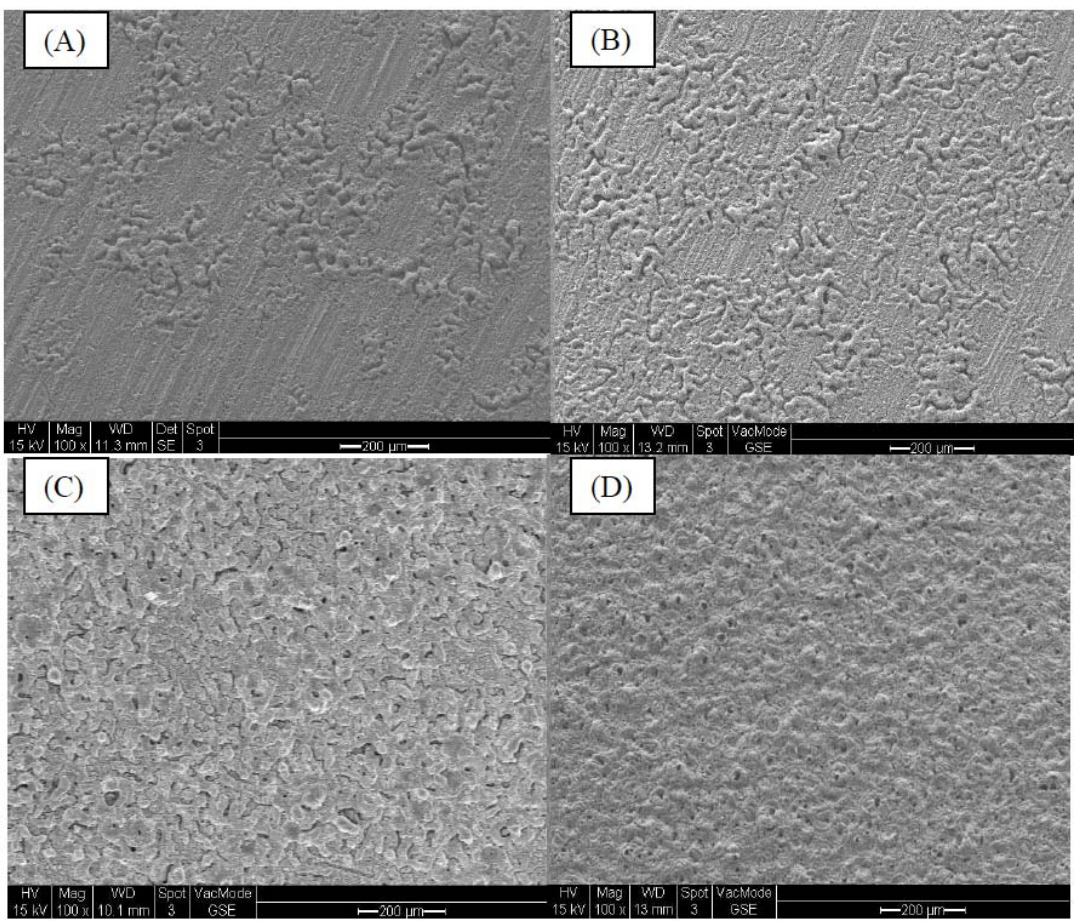

Figure 5: SEM of anodized AZ91D in various silicate concentration electrolytes. (**A**) 2 M NaOH + 0.05 M Na_2SiO_4 (A1); (**B**) 2 M NaOH + 0.15 M Na_2SiO_4 (A1-1); (**C**) 2 M NaOH + 0.5 M Na_2SiO_4 (A1-2); (**D**) 2 M NaOH + 3 M Na_2SiO_4 (A1-3).

Table 5: Detailed Surface Elements Information in Atom Percentage of Anodized AZ91D in Various Silicate Concentration Electrolytes. 2 M NaOH + 0.05 M Na_2SiO_4 (A1); 2 M NaOH + 0.15 M Na_2SiO_4 (A1-1); 2 M NaOH + 0.5 M Na_2SiO_4 (A1-2); 2 M NaOH + 3 M Na_2SiO_4 (A1-3)

	A1	A1-1	A1-2	A1-3
O	43.2	45.0	52.6	51.8
Na	-	1.8	6.7	16.7
Mg	51.3	46.1	26.5	9.4
Al	3.5	2.6	1.9	1.1
Si	2.0	4.5	12.3	21.0

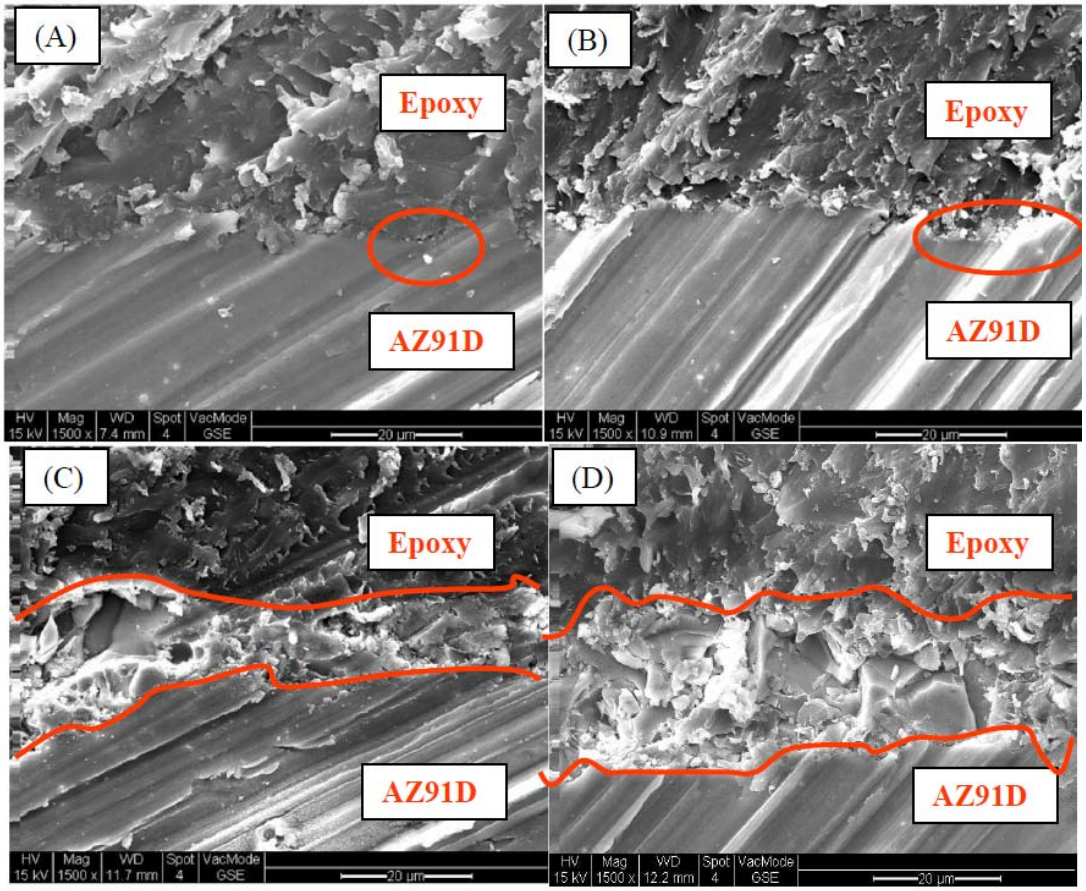

Figure 6: Cross-sections of of anodized AZ91D in various silicate concentration electrolytes. (**A**) 2 M NaOH + 0.05 M Na_2SiO_4 (A1); (**B**) 2 M NaOH + 0.15 M Na_2SiO_4 (A1-1); (**C**) 2 M NaOH + 0.5 M Na_2SiO_4 (A1-2); (**D**) 2 M NaOH + 3 M Na_2SiO_4 (A1-3).

DC polarization on samples of A1 and A1-3 was carried out after 10 hour immersion. The polarization curve is listed as Figure **7** and the fitting parameters are included in Table **4**. A1-3 showed better corrosion protective ability in terms of the lower corrosion rate. The corrosion rate of A1-3 was 2.01 mpy, but it was 5.79 mpy for A1. A1-3 also increased the corrosion potential compared to A1 from -1.42 V to -1.37 V.

4. DISCUSSION

The primary oxy-salts played an important role in anodizing AZ91D in alkaline electrolyte, in terms of the terminating voltage and anodizing behavior. The A0, A2, and A3 voltages first jumped and then dropped immediately due to a naturally formed magnesium oxide layer on the surface. At the start of anodization, the immediate effect of the increase in voltage was to break this first passivity film. However, the A1 voltage continued to increase, which indicated that the coating thickness and resistance also continued to increase. Adding silicate by forming Mg_2SiO_4, compared to phosphate and carbonate by forming MgO/Mg (OH) $_2$, helped the system build a thicker coating [4]. In the EDX measurements on A0, A1, A2 and A3, only Si was found in the coating. P and C were absent. This indicated that the high terminating

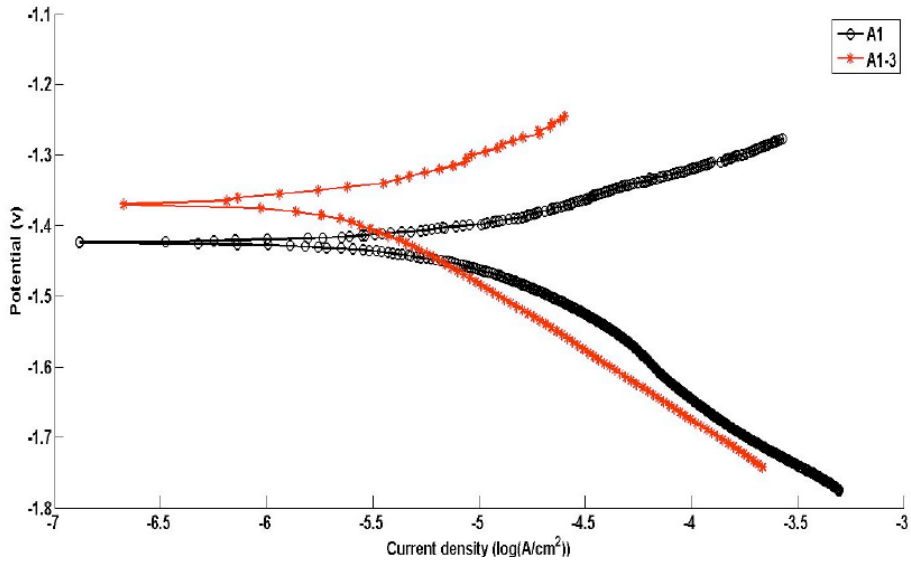

Figure 7: DC polarizatioin of A1 (2 M NaOH + 0.05 M Na_2SiO_4) and A1-3 (2 M NaOH + 3 M Na_2SiO_4) after 10 hours immersion in 0.15 M NaCl solution.

anodization voltage might be critical to the supportive functional oxy-salt formation. On the other hand, certain primary oxy-salts can help the thick coating to form and support high terminating voltage anodization. Therefore, selecting and adding the primary oxy-salts to the alkaline electrolyte is critical for different applications.

Our previous studies showed that the silicate could also increase the molar volume of the coating by forming Mg_2SiO_4 [4]. Contact angle measurements were made. The contact angle figures are listed in Figure **8**. And the summarized angles are in Table **6**. The fresh AZ91D had a contact angle of 68.9^o. A0, A2, A3 had no contact angles. Since A0, A2 and A3 coating generally had a ceramic composition of MgO/Mg $(OH)_2$; it lowered the coating hydrophobicity compared to the metal substrate. Moreover, the molar volume of MgO is smaller than that of Mg and this would cause the surface to shrink, generating a porous structure. However, A1 had a contact angle of 44.3^o of, and the presence of Si in the

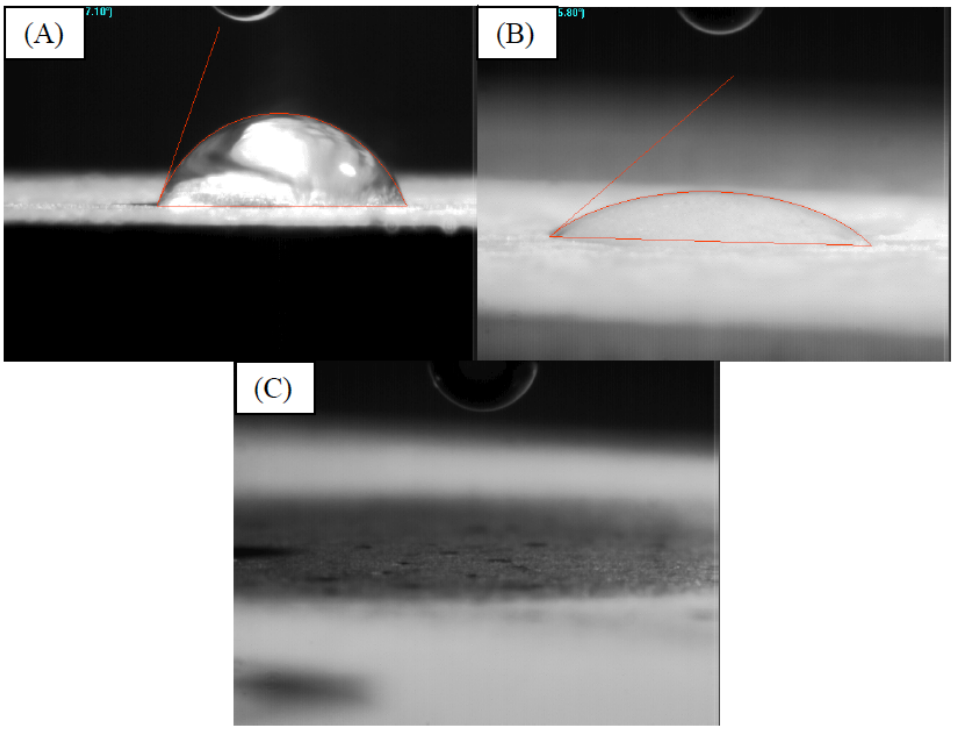

Figure 8: Contact angle images of anodized coatings from different primary oxy-salts addition electrolytes at 10 mA/cm^2 for 30 min. (**A**) Fresh AZ91D; (**B**) 2 M NaOH + 0.05 M Na_2SiO_3(A1); (**C**) 2 M NaOH(A0); 2 M NaOH + 0.05 M Na_3PO_4(A2); 2 M NaOH + 0.05 M Na_2CO_3(A3).

coating was the only difference from A0, A2 and A3. Mg_2SiO_4 might contribute to this difference. Mg_2SiO_4 has a higher molar volume, and it can help the coating smooth the shrinkage caused by formation of MgO [4, 20, 26]. Siloxane (-O-Si-O-) $(SiO_2)_x$ network deposited on the coating physically from the electrolyte might also increase the coating hydrophobicity [27-30].

Table 6: Contact Angle of Anodized Coatings from Different Primary Oxy-Salts Addition Electrolytes at 10 mA/cm^2 for 30 min. Fresh AZ91D; 2 M NaOH(A0); 2 M NaOH + 0.05 M Na_2SiO_3(A1); 2 M NaOH + 0.05 M Na_3PO_4(A2); 2 M NaOH + 0.05 M Na_2CO_3(A3)

	Contact angle
AZ91D	68.9^o
A0	0
A1	44.3^o
A2	0
A3	0

5. CONCLUSIONS

Silicate, phosphate, and carbonate primary oxy-salts were added to a sodium hydroxide alkaline electrolyte used for anodization. SEM and EDX characterized the surface. Electrochemical tests in 0.15 M NaCl solution were used to evaluate the anodized coating. The results and findings obtained from this work are listed as follows:

1) Different oxy-salts could lead to different anodization behavior.

2) Adding silicate increased the anodization terminating voltage, generated sparks, and helped the system to build a thicker and more corrosion resistant coating.

3) A high concentration of silicate in the electrolyte, but below its solubility limit, yielded a smooth film with small pore size, low porosity, and a thick, corrosion resistant coating.

ACKNOWLEDGEMENTS

This work is sponsored by the National Science Foundation (NSF) Engineering Research Center (ERC) for Revolutionizing Metallic Biomaterials (RMB). This support is gratefully acknowledged.

REFERENCES

[1] Witte F, Fischer J, Nellesen J, *et al*. *In vitro* and *in vivo* corrosion measurements of magnesium alloys. Biomaterials 2006; 27(7): 1013-18. http://dx.doi.org/10.1016/j.biomaterials.2005.07.037

[2] Witte F, Kaese V, Haferkamp H, *et al*. *In vivo* corrosion of four magnesium alloys and the associated bone response. Biomaterials 2005; 26(17): 3557-63. http://dx.doi.org/10.1016/j.biomaterials.2004.09.049

[3] Zeng RC, Dietzel W, Witte F, Hort N, Blawert C. Progress and challenge for magnesium alloys as biomaterials. Adv Eng Mater 2008; 10(8): B3-B14. http://dx.doi.org/10.1002/adem.200800035

[4] Xue D, Yun Y, Schulz MJ, Shanov V. Corrosion protection of biodegradable magnesium implants using anodization. Mater Sci Eng C 2011; 31(2): 215-23. http://dx.doi.org/10.1016/j.msec.2010.08.019

[5] Hiromoto S, Shishido T, Yamamoto A, Maruyama N, Somekawa H, Mukai T. Precipitation control of calcium phosphate on pure magnesium by anodization. Corrosion Sci 2008; 50(10): 2906-13. http://dx.doi.org/10.1016/j.corsci.2008.08.013

[6] Khaselev O, Yahalom J. The anodic behavior of binary Mg-Al alloys in KOH-aluminate solutions. Corrosion Sci 1998; 40(7): 1149-60. http://dx.doi.org/10.1016/S0010-938X(98)00019-5

[7] Mizutani Y, Kim SJ, Ichino R, Okido M. Anodizing of Mg alloys in alkaline solutions. Surface Coat Technol 2003; 169: 143-46. http://dx.doi.org/10.1016/S0257-8972(03)00214-7

[8] Li LL, Cheng YL, Wang HM, Zhang Z. Anodization of AZ91 magnesium alloy in alkaline solution containing silicate and corrosion properties of anodized films. Trans Nonferrous Metals Soc China 2008; 18(3): 722-27. http://dx.doi.org/10.1016/S1003-6326(08)60124-7

[9] Ono S, Miyake M, Asoh H. Effects of formation voltage and electrolyte ions concentration on the structure and passivity of anodic films on magnesium. J Jpn Instit Light Metals 2004; 54(11): 544-50. http://dx.doi.org/10.2464/jilm.54.544

[10] Hsiao HY, Tsai WT. Characterization of anodic films formed on AZ91D magnesium alloy. Surf Coat Technol 2005; 190(2-3): 299-308. http://dx.doi.org/10.1016/j.surfcoat.2004.03.010

[11] Park IS, Jang YS, Kim Y K, Lee MH, Yoon JM, Bae TS. Surface characteristics of AZ91D alloy anodized with various conditions. Surf Interf Anal 2008; 40(9): 1270-77. http://dx.doi.org/10.1002/sia.2876

[12] Barchiche CE, Rocca E, Juers C, Hazan J, Steinmetz J. Corrosion resistance of plasma-anodized AZ91D magnesium alloy by electrochemical methods. Electrochim Acta 2007; 53(2): 417-25. http://dx.doi.org/10.1016/j.electacta.2007.04.030

[13] Ghasemi A, Raja VS, Blawert C, Dietzel W, Kainer KU. The role of anions in the formation and corrosion resistance of the plasma electrolytic oxidation coatings. Surf Coat Technol 2010; 204(9-10): 1469-78. http://dx.doi.org/10.1016/j.surfcoat.2009.09.069

[14] Wen Q, Cao FH, Shi YY, Zhang Z, Zhang JQ. The effect of phosphate on MAO of AZ91D magnesium using AC power source. Materials and Corrosion-Werkstoffe Und Korrosion 2008; 59(10): 819-24. http://dx.doi.org/10.1002/maco.200804169

[15] Salman S, Ichino R, Okido M. Influence of calcium hydroxide and anodic solution temperature on corrosion property of anodising coatings formed on AZ31 Mg alloys. Surf Eng 2008; 24(3): 242-45. http://dx.doi.org/10.1179/174329408X282578

[16] Birss V, Xia S, Yue R, Rateick RG. Characterization of oxide films formed on Mg-based WE43 alloy using AC/DC anodization in silicate solutions. J Electrochem Soc 2004; 151(1): B1-B10. http://dx.doi.org/10.1149/1.1629095

[17] Zhang YJ, Yan CW, Wang FH, Lou HY, Cao CN. Study on the environmentally friendly anodizing of AZ91D magnesium alloy. Surf Coat Technol 2002; 161(1): 36-43. http://dx.doi.org/10.1016/S0257-8972(02)00342-0

[18] Duan HP, Yan CW, Wang FH. Growth process of plasma electrolytic oxidation films formed on magnesium alloy AZ91D in silicate solution. Electrochim Acta 2007; 52(15): 5002-5009. http://dx.doi.org/10.1016/j.electacta.2007.02.021

[19] Guo HF, An MZ, Huo HB, Xu S, Wu LJ. Microstructure characteristic of ceramic coatings fabricated on magnesium alloys by micro-arc oxidation in alkaline silicate solutions. Appl Surf Sci 2006; 252(22): 7911-16. http://dx.doi.org/10.1016/j.apsusc.2005.09.067

[20] Wu HL, Cheng YL, Li LL, Chen ZH, Wang HM, Zhang Z. The anodization of ZK60 magnesium alloy in alkaline solution containing silicate and the corrosion properties of the anodized films. Appl Surf Sci 2007; 253(24): 9387-94. http://dx.doi.org/10.1016/j.apsusc.2007.05.085

[21] Fukuda H, Matsumoto Y. Effects of Na2SiO3 on anodization of Mg-Al-Zn alloy in 3 M KOH solution. Corrosion Sci 2004; 46(9): 2135-42. http://dx.doi.org/10.1016/j.corsci.2004.02.001

[22] Chai LY, Yu X, Yang ZH, Wang YY, Okido M. Anodizing of

magnesium alloy AZ31 in alkaline solutions with silicate under continuous sparking. Corrosion Sci 2008; 50(12): 3274-79. http://dx.doi.org/10.1016/j.corsci.2008.08.038

[23] Zhao M, Wu S, An P, Luo J. Study on the deterioration process of a chromium-free conversion coating on AZ91D magnesium alloy in NaCl solution. Appl Surf Sci 2006; 253(2): 468-75. http://dx.doi.org/10.1016/j.apsusc.2005.12.122

[24] Liang J, Srinivasan PB, Blawert C, Dietzel W. Influence of chloride ion concentration on the electrochemical corrosion behaviour of plasma electrolytic oxidation coated AM50 magnesium alloy. Electrochim Acta 2010; 55(22): 6802-11. http://dx.doi.org/10.1016/j.electacta.2010.05.087

[25] Duan H, Du K, Yan C, Wang F. Electrochemical corrosion behavior of composite coatings of sealed MAO film on magnesium alloy AZ91D. Electrochim Acta 2006; 51(14): 2898-908. http://dx.doi.org/10.1016/j.electacta.2005.08.026

[26] Zhang YJ, Yan CW. Development of anodic film on Mg alloy AZ91D. Surf Coat Technol 2006; 201(6): 2381-86. http://dx.doi.org/10.1016/j.surfcoat.2006.04.015

[27] van Ooij WJ, Zhu D, Stacy M, Seth A, Mugada T, Gandhi J, Puomi P. Corrosion Protection Properties of Organofunctional Silanes--An Overview. Tsinghua Sci Technol 2005; 10(6): 639-64. http://dx.doi.org/10.1016/S1007-0214(05)70134-6

[28] Montemor MF, Ferreira MGS. Analytical and microscopic characterisation of modified bis-[triethoxysilylpropyl] tetrasulphide silane films on magnesium AZ31 substrates. Progr Organ Coat 2007; 60(3): 228-37. http://dx.doi.org/10.1016/j.porgcoat.2007.07.019

[29] Montemor MF, Ferreira MGS. Electrochemical study of modified bis-[triethoxysilylpropyl] tetrasulfide silane films applied on the AZ31 Mg alloy. Electrochim Acta 2007; 52(27): 7486-95. http://dx.doi.org/10.1016/j.electacta.2006.12.086

[30] Kim J, Wong KC, Wong PC, Kulinich SA, Metson JB, Mitchell KAR. Characterization of AZ91 magnesium alloy and organosilane adsorption on its surface. Appl Surf Sci 2007; 253(9): 4197-207. http://dx.doi.org/10.1016/j.apsusc.2006.09.030